17. Heteronuclear Shift Correlations

The correlation of the chemical shifts of heteronuclei is usually accomplished by the detection of the more sensitive proton spin. Since the time when this technique was introduced by Mueller,[1] a number of variants have been developed.[32,2,3,4,5,6]

17.1 Heteronuclear Multiple Quantum Correlation (HMQC)

Figure 17.1.1 shows the pulse sequence and the associated CFN for the Heteronuclear Multiple Quantum Correlation (HMQC) experiment.[7] Two different radiofrequency channels are used in this experiment, one for the **I** spin and one for the **S** spin. The RF pulses are independently generated and excitation of the **I** spins has no effect on the **S** spin and *vice versa*. This experiment correlates the chemical shift of the **I** spin to the chemical shift of a scalar coupled **S** spin. Typically, the **I** spin is a proton that has a large single bond coupling constant to the **S** spin, usually either a ^{15}N or ^{13}C nucleus.

The sequence begins with the excitation of the **I** spin by a 90° degree pulse. The evolution <A,B> serves to build up the antiphase $\mathbf{2I_xS_z}$ state at <B>. During the <A,B> evolution there is **I** spin chemical shift evolution; however, the 180° pulse at the center of the <B,E> period refocuses the chemical shift of the **I** spin over the entire <A,F> interval. On average, there is no chemical shift evolution of the **I** spins except during detection, <F,G>. The absence of chemical shift (on average) is represented in the CFN by the horizontal line <A,B,E,F>. At <B,C> a 90° pulse is applied to the **S** spin and precession begins at the **S** chemical shift frequency. During the t_1 period both of the correlated **I** and **S** spins are transverse. This multiple quantum coherence would normally precess at the sum and difference of the frequencies of the spins involved in the coherence; as remarked above, however, on average there is no precession of the **I** spin and therefore the multiple quantum coherence is labeled only with the frequency of the **S** spin during <C,D>. The second 90° **S** pulse at <D,E> recreates the $\mathbf{2I_xS_z}$ antiphase state at <E> that is now frequency labeled with the **S** chemical shift. The <E,F> period serves to refocus the antiphase state into $\mathbf{I_y}$ at <F> which is then detected during <F,G> with **S** nucleus decoupling.

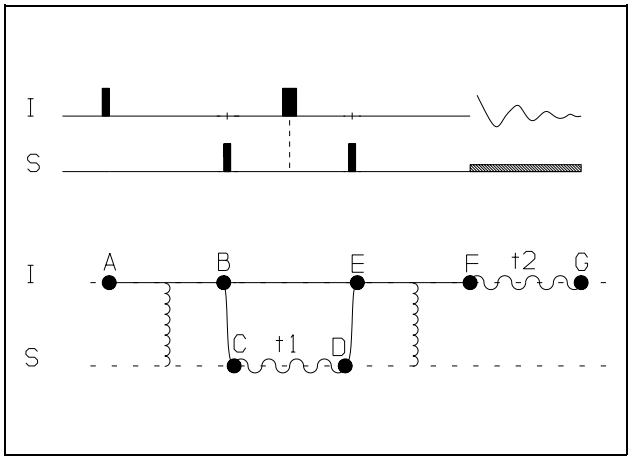

Figure 17.1.1. Pulse sequence and CFN for Heteronuclear Multiple Quantum Correlation (HMQC) spectroscopy.

Preparation:

$\mathbf{I}_z \ = \pi/2\hat{\mathbf{I}}_x \Rightarrow -\mathbf{I}_y$ (17.1.1)

$-\mathbf{I}_y \ = \pi J_{IS} t 2\hat{\mathbf{I}}_z\hat{\mathbf{S}}_z \Rightarrow -\mathbf{I}_y \cos \pi J_{IS} t + 2\mathbf{I}_x\mathbf{S}_z \sin \pi J_{IS} t$ (17.1.2)

With $t = 1/(2J_{IS})$, $\cos \pi J_{IS} t = 0$ and $\sin \pi J_{IS} t = 1$, the state at <B> (Eqn. 17.1.2) becomes,

$2\mathbf{I}_x\mathbf{S}_z$ (17.1.3)

Evolution:

The π/2 pulse on the **S** spins yields a coherence in which both spins are transverse. This is a superposition of zero and double quantum coherence.

$2\mathbf{I}_x\mathbf{S}_z \ = \pi/2\hat{\mathbf{S}}_x \Rightarrow -2\mathbf{I}_x\mathbf{S}_y$ (17.1.4)

This coherence evolves only under the chemical shift of the **S** spin due to the refocusing effect of the 180° pulse on the **I** spin (Eqns. 17.1.5-17.1.7)

$-2\mathbf{I}_x\mathbf{S}_y = \omega_S t_1/2\hat{\mathbf{S}}_z \Rightarrow -2\mathbf{I}_x\mathbf{S}_y \cos \omega_S t_1/2 + 2\mathbf{I}_x\mathbf{S}_x \sin \omega_S t_1/2$ (17.1.5)

$= \pi\hat{\mathbf{I}}_x \Rightarrow -2\mathbf{I}_x\mathbf{S}_y \cos \omega_S t_1/2 + 2\mathbf{I}_x\mathbf{S}_x \sin \omega_S t_1/2$ (17.1.6)

$= \omega_S t_1/2\hat{\mathbf{S}}_z \Rightarrow -2\mathbf{I}_x\mathbf{S}_y \cos \omega_S t_1 + 2\mathbf{I}_x\mathbf{S}_x \sin \omega_S t_1.$ (17.1.7)

The second **S** π/2 pulse recreates antiphase coherence labeled by the frequency of the **S** spin

$= \pi/2\hat{\mathbf{S}}_x \Rightarrow \ -2\mathbf{I}_x\mathbf{S}_z \cos \omega_S t_1 + 2\mathbf{I}_x\mathbf{S}_x \sin \omega_S t_1.$ (17.1.8)

$2\mathbf{I}_x\mathbf{S}_x$ is unobservable and can be neglected. Further evolution under coupling gives,

$= \pi J_{IS} t 2\hat{\mathbf{I}}_z\hat{\mathbf{S}}_z \Rightarrow \ (-2\mathbf{I}_x\mathbf{S}_z \cos \pi J_{IS} t - \mathbf{I}_y \sin \pi J_{IS} t) \cos \omega_S t_1$ (17.1.9)

Again with $t = 1/(2J_{IS})$, one obtains

$= \ -\mathbf{I}_y \cos \omega_S t_1.$ (17.1.10)

Detection:

With **S** nucleus decoupling, the only evolution during detection is due to **I** chemical

shift.

$$-\mathbf{I}_y \cos \omega_s t_1 \exp(i \omega_I t_2) \qquad (17.1.11)$$

With quadrature detection in ω_1 and hypercomplex Fourier transform, the two-dimensional spectrum consists of peaks located at the intersection of the chemical shifts of the scalar coupled I and S spins (as in Figure 5.1.4).

17.2 HMQC Phase Cycling

For heteronuclei, nuclear-spin selective pulses do not effect the evolution of the heteronucleus. For this reason, the phase cycling is done independently.

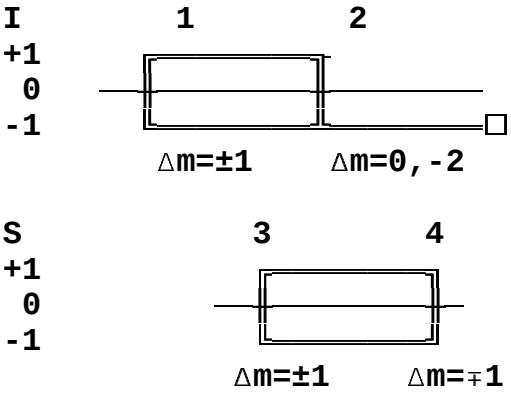

Performing the necessary phase calculations:

I ϕ_1:	**I** ϕ_2:	**S** ϕ_3:	**S** ϕ_4:
Δm=±1	Δm=0,-2	Δm=±1	Δm=∓1
+1 (0 **-1**)	(**-2** -1) 0 1 2	-1 (0 **+1**)	-1 (0 **+1**)
N=2	N=2	N=2	N=2
ϕ_1 = 0 π	ϕ_2 = 0 π	ϕ_3 = 0 π	ϕ_4 = 0 π

To remove quadrature images, the **I** channel can be further constrained to allow only Δm=-1 for the entire sequence. This phase cycle is the CYCLOPS procedure of Section 3.9. With the CYCLOPS sequence superimposed on the rest of the **I** channel phase cycle gives a 64 step phase cycle. Again, note that the **S** channel is treated independently.

64 step phase table for HMQC:

ϕ_1: 8(0,π) 8(π/2,3π/2) 8(π,0) 8(3π/2,π/2)
ϕ_2: 4(0,0,π,π) 4(π/2,π/2,3π/2,3π/2) 4(π,π,0,0) 4(3π/2,3π/2,π/2,π/2)

ϕ_3: 8(0,0,0,0,π,π,π,π)
ϕ_4: 4(0,0,0,0,0,0,0,0,π,π,π,π,π,π,π,π)
ψ: (0,π,π,0,π,0,0,π,π,0,0,π,0,π,π,0)
(3π/2,π/2,π/2,3π/2,π/2,3π/2,3π/2,π/2,π/2,3π/2,3π/2,π/2,3π/2,π/2,π/2,3π/2)
(π,0,0,π,0,π,π,0,0,π,π,0,π,0,0,π)
(π/2,3π/2,3π/2,π/2,3π/2,π/2,π/2,3π/2,3π/2,π/2,π/2,3π/2,π/2,π/2,3π/2,3π/2,π/2)

This represents a complete phase cycle for the HMQC experiment. One major disadvantage is the number of experiments necessary to accomplish the full phase cycle. A modest size for a two dimensional experiment would be to collect 512 points along t_1. If the recycle time for each scan is 1 s then the minimum time for an HMQC experiment would be 1 X 64 X 512 = 32768 seconds or about 9 hours. The sensitivity of this experiment for a fully ^{13}C or ^{15}N labeled sample (the **S** nucleus) is very nearly the sensitivity obtained for ^1H (the **I** spin) alone. A sample of 1-2 mM concentration gives good signal-to-noise for ^1H spectra at 500 MHz in a very short period of time (< 5 minutes). Ideally, the 2D experiment should only take a few minutes, but with full phase cycling the time is enormously increased. An obvious solution is not to do the complete phase cycle. The first luxury to be eliminated is the CYCLOPS routine which eliminates quadrature images. If the spectrometer receiver is adjusted properly, the amplitude of the quadrature images should be less than 1% of the real signal. Eliminating this step of the phase cycle reduces the number of required scans by a factor of 4. This still means that the experiment will take a little more than 2 hours to collect. Heteronuclear experiments are unique in that the RF pulses applied to one spin do not effect the heteronuclear spin. The part of the phase cycle in which the **S** spin pulse phase is inverted along with the inversion of the receiver eliminates any **I** coherence that is not part of a heteronuclear spin coherence. This selects only **I** spins that are coupled to **S** spins and eliminates all other uncoupled **I** spins, which are unmodulated by the heteronuclear coupling. This spectral editing feature is very effective as a phase cycling step. Applying the most severe reduction of phase cycling, each t_1 block of the HMQC experiment can be obtained by 2 acquisitions.

ϕ_3 0 π
ψ 0 π

This reduces the experimental time to about 20 minutes. More rapid accumulations can made by reducing the resolution in the t_1 dimension or reducing the recycle time.

The steps in a phase cycle that can be eliminated or truncated are not always obvious. As a rule of thumb, in a heteronuclear sequence, the two step phase cycle of the non-observed nucleus that inverts the coherence and thus inverts the receiver is the simplest sequence. Additional phase cycles on the observed or unobserved nucleus that are the next most efficient depend the particular type of artifacts that are to be removed.

17.3 Modulation from ^{1}H-^{1}H scalar coupling

In most cases there will be other spins (**I'**) in the molecule under study that are coupled to **I**. During the t_1 period, **I-I'** coupling is active, and the **S** spin is modulated by cos ($\pi J_{II'} t_1$) during the t_1 period (Figure 17.3.1). If the t_1 period is kept short compared to the reciprocal of the small **I-I'** coupling constant, the passive coupling will not influence the **S** signal to any great extent. However, in order to increase the frequency resolution in the **S** dimension, the t_1 period must be lengthened. The result of this passive coupling during t_1 is that the peak is split along the ω_S dimension by $J_{II'}$. This method has been used to obtain $^{3}J_{\alpha\beta}$ ^{1}H coupling constants in ^{15}N labeled proteins.

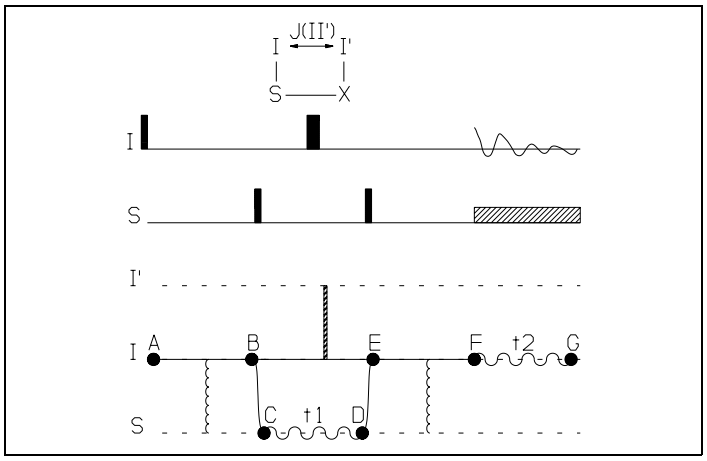

Figure 17.3.1. HMCQ pulse sequence with CFN showing passive **II'** coupling.

17.4. Heteronuclear Single Quantum Correlation (HSQC)

Figure 17.4.1 shows the pulse sequence and CFN for Heteronuclear Single Quantum Correlation (HSQC).[29] Like HMQC, this sequence is used for the chemical shift correlation of **I** and **S** nuclei with different magnetogyric ratios. The sequence consists of a pair of symmetric transfer steps that surround the chemical shift evolution period of the S nucleus. After the first 90° pulse on the **I** spin at <A>, the system evolves by heteronuclear scalar coupling to a heteronuclear antiphase state, $\mathbf{2I_xS_z}$, at <B>. Coherence transfer occurs along <B,C> and at <C> the state of the system is $\mathbf{2I_zS_y}$. The antiphase state at <C> is refocused into pure $-\mathbf{S_x}$

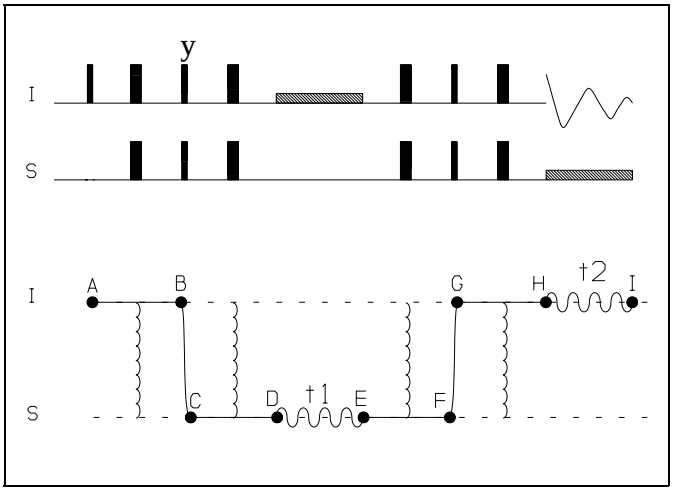

Figure 17.4.1. Pulse sequence and CFN for Heteronuclear Single Quantum Spectroscopy. This particular experiment is a double refocused INEPT type transfer.

coherence during <C,D>. Frequency labeling of the **S** spin occurs during the t_1 period <D,E>. The **IS** scalar coupling interaction is removed during <D,E> by continuous broadband spin decoupling of the **I** spin. The decoupling can be accomplished also by replacing the broadband decoupling sequence with a single 180° pulse at the center of the t_1 period. The resulting **S** resonance is slightly narrower in the sequence using broadband decoupling. From the end of the t_1 period, the sequence consists of a mirror image of the <A,D> path. Antiphase coherence is obtained during <E,F>, coherence transfer occurs across <F,G>, and the resulting antiphase state is refocused into pure **I** spin coherence during <G,H> for detection during t_2 (<H,I>).

Using product operator analysis, the first pulse generates

$$\mathbf{I}_z \ =\pi/2\hat{\mathbf{I}}_x\Rightarrow -\mathbf{I}_y \qquad (17.4.1)$$

The sequence of a delay followed by a 180° pulse on the x axis (phase equal to zero) on both coupled nuclei followed by the same delay can be represented as a single rotation (Table 2.1B).

$$=\pi J_{IS}\Delta\mathbf{2}\hat{\mathbf{I}}_z\hat{\mathbf{S}}_z\Rightarrow \qquad (17.4.2)$$

If Δ is $1/(2J_{IS})$, then the sequence <A,B> becomes:

$$\mathbf{I}_z \ =\pi/2\hat{\mathbf{I}}_x\Rightarrow -\mathbf{I}_y \ =\pi/2_{IS}\mathbf{2}\hat{\mathbf{I}}_z\hat{\mathbf{S}}_z\Rightarrow \mathbf{2I}_x\mathbf{S}_z. \qquad (17.4.3)$$

Simultaneous (or nearly so) 90° pulses on both nuclei effect the coherence transfer, <B,C>

$$\mathbf{2I}_x\mathbf{S}_z \ =\pi/2(\hat{\mathbf{I}}_y+\hat{\mathbf{S}}_x)\Rightarrow \mathbf{2I}_z\mathbf{S}_y. \qquad (17.4.4)$$

Note that the phase of the **I** pulse at <B> is 90° out of phase with respect to the first 90° **I** pulse. The sequence <C,D> can be simplified to

$$\mathbf{2I}_z\mathbf{S}_y \ =\pi J_{IS}\Delta\mathbf{2}\hat{\mathbf{I}}_z\hat{\mathbf{S}}_z\Rightarrow -\mathbf{S}_x. \qquad (17.4.5)$$

During the t_1 period, the **S** coherence is frequency labeled,

$$-\mathbf{S}_x \ =\omega_S t_1\hat{\mathbf{S}}_z\Rightarrow -\mathbf{S}_x\cos\omega_S t_1 - \mathbf{S}_y\sin\omega_S t_1 \qquad (17.4.6)$$

During <E,F>, the **S** transverse magnetization evolves into an antiphase state. Using the composite rotation from Eqn 17.4.2, we obtain

$$-\mathbf{S}_x\cos\omega_S t_1 - \mathbf{S}_y\sin\omega_S t_1 =\pi J_{IS}\Delta\mathbf{2}\hat{\mathbf{I}}_z\hat{\mathbf{S}}_z\Rightarrow \ -\mathbf{2I}_z\mathbf{S}_y\cos\omega_S t_1 + \mathbf{2I}_z\mathbf{S}_x\sin\omega_S t_1. \qquad (17.4.7)$$

Coherence transfer occurs at <F,G> upon the application of 90° pulses to both spins.

$$-2I_zS_y \cos \omega_s t_1 + 2I_zS_x \sin \omega_s t_1 \;\; =\pi/2(\hat{I}_x+\hat{S}_x)=>$$
$$2I_yS_z \cos \omega_s t_1 - 2I_yS_x \sin \omega_s t_1 \qquad (17.4.8)$$

Only the $2I_yS_z$ term will evolve into observable magnetization since the $2I_yS_x$ term is a superposition of heteronuclear multiple quantum states.

During <G,H> the antiphase state refocuses into observable **I** magnetization

$$2I_yS_z \cos \omega_s t_1 = \pi J_{IS} \Delta 2\hat{I}_z\hat{S}_z => -I_x \cos \omega_s t_1. \qquad (17.4.9)$$

The detection period consisting of chemical shift on the **I** spins during <H,I> yields

$$-I_x \cos \omega_s t_1 \, e^{i\omega(I)t} \qquad (17.4.10)$$

17.5 Coherence Transfer Pathway and Phase Cycling for HSQC

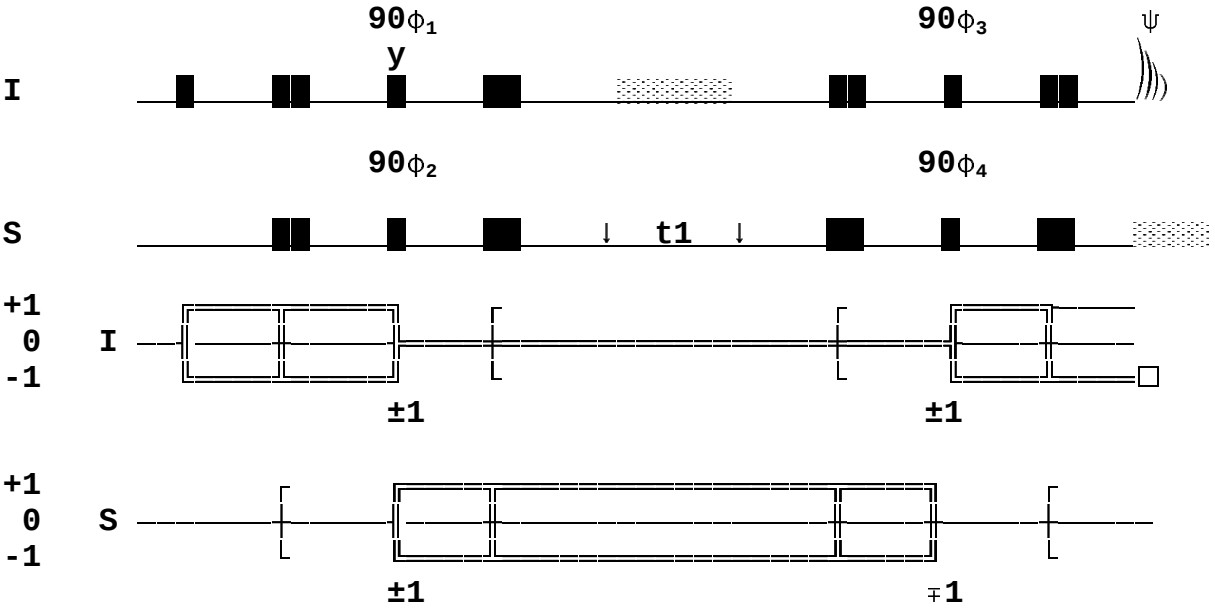

A computation of the number of phase shifted experiments required for this sequence yields more than 8000 if all pulses are fully cycled. Obviously, this is not very practical. The pulses (ϕ_1..ϕ_4) that are marked in the above pulse sequence constitute editing steps. These steps involve the inversion of the coherence of interest followed by the subtraction of the resultant signal in the computer memory.

Consider the 90° pulse with phase ϕ_2 at the coherence transfer step <B,C>. The standard analysis for the phase cycle yields:

ϕ_2:
$\Delta m=\pm 1$
(**1** 0) **-1**
N=2
$\phi_2 = 0,\pi$

For the coherence at <B> (Figure 17.4.1), applying a 90° $\mathbf{S}_x$ and a 90° $\mathbf{I}_y$ pulse yields

$$\mathbf{2I_xS_z} \ =\pi/2(\hat{I}_y+\hat{S}_x)=> \mathbf{2I_zS_y}. \qquad (17.5.1)$$

Eventually this leads to the detected signal

$$-\mathbf{I}_x \cos \omega_S t_1. \qquad (17.5.2)$$

Inverting the phase of the **S** pulse (-90° $\mathbf{S}_x$) changes the sign of the coherence;

$$\mathbf{2I_xS_z} \ =\pi/2\hat{I}_y-\pi/2\hat{S}_x=> \mathbf{-2I_zS_y} \qquad (17.5.3)$$

leading to a detected signal of opposite sign.

$$\mathbf{I}_x \cos \omega_S t_1 \qquad (17.5.4)$$

In order to have constructive interference, the signals from these two steps in the phase cycle the two signal must be subtracted. Any other **I** coherence that is not in an antiphase state with **S** will not be inverted in either sequence and any resultant observable signal will be subtracted away. For example, if there is a spin $\mathbf{I}'$, which is not coupled to an **S** spin, its behavior at step <B,C> will be:

$$\mathbf{I}'_y =\pi/2(\hat{I}'_y+\hat{S}_x)=> \mathbf{I}'_y \qquad (17.5.5)$$

and

$$\mathbf{I}'_y =\pi/2\hat{I}'_y-\pi/2\hat{S}_x=> \mathbf{I}'_y \qquad (17.5.6)$$

Any part of this $\mathbf{I}'$ signal, which ultimately reaches the receiver, will be removed by subtraction.

The CTP analysis for all of the other 90° pulses is identical to this one since all of the changes on coherence order are ±1 (or $\mp$1). The same effect is obtained by inverting the **I** pulse at step <B,C>.

$$\mathbf{2I_xS_z} \ =-\pi/2\hat{I}_y+\pi/2\hat{S}_x=> \mathbf{-2I_zS_y} \qquad (17.5.7)$$

and the resulting signal will be subtracted from the first experiment [=π/2($\hat{\mathbf{I}}_y$+$\hat{\mathbf{S}}_x$)=>] and added to the result from the second phase cycle step [=π/2$\hat{\mathbf{I}}_y$-π/2$\hat{\mathbf{S}}_x$=>]. The phase table for this experiment with only the 90° pulses cycled gives a phase cycle with a length of 16 scans.

ϕ_1: 2(0) 2(π)
ϕ_2: 8(0 π)
ϕ_3: 8(0) 8(π)
ϕ_4: 4(0) 4(π)
ψ: (0 π π 0) 2(π 0 0 π) (0 π π 0)

All of the other pulses in this sequence, except for the initial 90° pulse, are 180° pulses. These pulses are rather sensitive to off-resonance effects. There are two different types of phase cycling schemes that are usually employed for 180° pulses depending on whether the magnetization is transverse or longitudinal. For 180° pulses used to invert Z magnetization, the phase can be cycled in 90° steps without changing the receiver phase (Section 3.11). For transverse magnetization EXORCYCLE is used; this phase cycle consists of 90° phase increments associated with phase inversion of the receiver. To shorten the length of the experiment, often the phases of 180° pulses are simply inverted without any changing the receiver phase.

The quality of 180° degree pulses used to invert Z magnetization can be improved by using composite pulses of the type 90_x:180_y:90_x or 90_x:180_{-x}:270_x. This may lead to greater sensitivity in certain experiments. Special care must be taken in applying composite 180° pulses to transverse magnetization and this procedure is not generally recommended without detailed analysis.

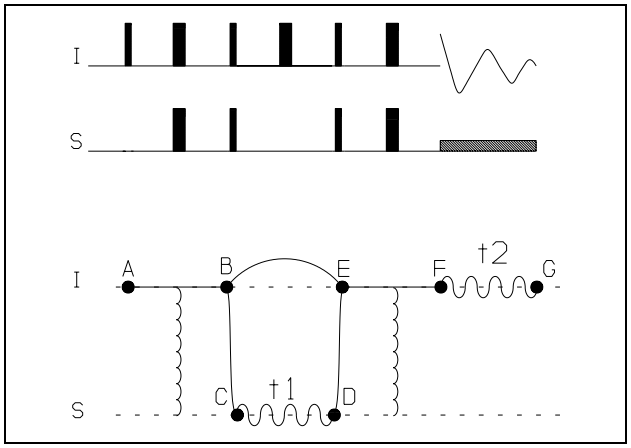

Figure 17.6.1. Pulse sequence and CFN for a HSQC experiment with evolution of **S** antiphase with respect to **I**.

17.6 Variations on HSQC

The HSQC experiment can also be collected with the pulse sequence shown in Figure 17.6.1. The main difference between this sequence and the experiment described in Figure 17.4.1 is that the antiphase signal, $\mathbf{2I_zS_y}$, at state <C> is not refocused into $\mathbf{S_x}$. The refocusing step is eliminated on both sides of the t_1 period and the chemical shift evolution of the **S** spin occurs as an antiphase state during <C,D>. The Z primitive (Table 1.1) that connects states <B> and <E> represents the retention

of the antiphase state during this period. The 180° pulse in the center of <C,D> is a decoupling pulse, which replaces the broadband decoupling sequence shown in Figure 17.4.1. In detail, the use of a decoupling sequence, such as WALTZ or MLEV, prevents oscillation between antiphase and inphase states, whereas a single 180° pulse permits antiphase to inphase oscillation during <B,E> with the antiphase state returned at <E>. This difference becomes important if the relaxation of the of the antiphase state is of interest. The oscillation between antiphase and inphase states will allow transverse relaxation from both states. This will be manifested as a superposition of **S** resonances with different linewidths. In this sequence, if a broadband decoupling cycle is used then care must be taken to assure that the **I** spins are returned to the Z axis at <E>.

Another variation of heteronuclear shift correlation experiments is heteronuclear single- and multiple-quantum correlation (HSMQC)[31]. HSMQC is a combination of HMQC and HSQC, which provides improved sensitivity by the elimination of coupling to remote protons. Essentially, this technique superimposes HMQC and HSQC cross peaks.

An enormous reduction in the time required to collect HSQC spectra can be achieved by the use of pulsed field gradients (PFG). The number of acquisitions required per t_1 increment can be lowered to one. The HSQC experiment lends itself very nicely to the use of PFGs since there are a number of "sites" in the pulse sequence where they can be incorporated. The two especially vulnerable sites are at the points of heteronuclear coherence transfer. By the proper placement of the ^{1}H and the X pulses, a longitudinal two-spin order state $\mathbf{2I_zS_z}$ can be created. The coherence order of this state is zero and thus has no dependence on a phase shift. Since these points are editing steps of this sequence, only the desired magnetization passes the PFG spoilers. Another advantage of the use of PFGs is that since the diffusion coefficient for water is much larger than that for a macromolecule, the water resonance can be effectively eliminated without the use of presaturation. Any loss of intensity of amide proton signals due to saturation transfer from water and any intensity losses due to spin diffusion from saturated α protons having the same chemical shift as water can be circumvented.

One possible placement of the PFGs in the HSQC experiment is shown below.

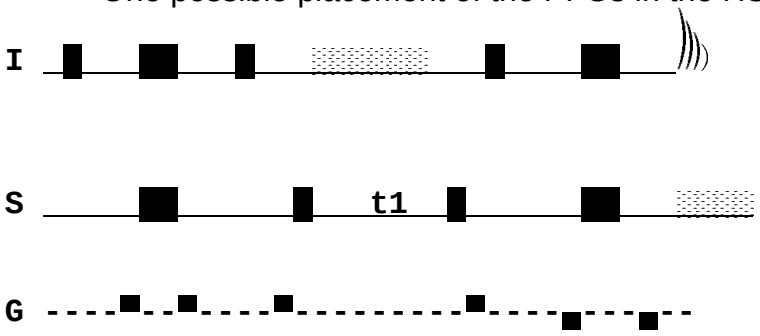

The PFGs surrounding the 180° pulses were discussed in Section 10.10.

1. L. Mueller (1979) *J. Am. Chem. Soc.* **101**, 4481.

2. A. Bax, R. H. Griffey, and B. L. Hawkins (1983) *J. Am. Chem. Soc.* **105**, 7188.

3. M. R. Bendall, D. T. Pegg, and D. M. Doddrell (1983) *J. Magn. Reson.* **52**, 81.

4. G. Bodenhausen and D. J. Ruben (1980) *Chem. Phys. Lett.* **69**, 185.

5. A. G. Redfield (1983) *Chem. Phys. Lett.* **96**, 537.

6. E. R. P. Zuiderweg (1990) *J. Magn. Reson.* **86**, 346.

7. A. Bax, R. H. Griffey, and B. L. Hawkins (1983) *J. Magn. Reson.* **55**, 301.